molbank

MDPI

Communication

Development of New Aryl-Substituted 1,2,3-Triazole Derivatives of Celastrol: Synthetic Approaches and Structural Characterization

Yuhan Xie [1], Nayara Macêdo Peixoto Araujo [2], Stanislau Bogusz Junior [3], Deepa Alex [4] and Paolo Coghi [1,5,*]

[1] School of Pharmacy, Macau University of Science and Technology, Macau 999078, China; 2240026307@student.must.edu.mo
[2] Graduate Program in Food Science and Technology, Institute of Technology, Federal University of Pará, Belem 66075-110, PA, Brazil; nayarapeixoto@ufpa.br
[3] São Carlos Institute of Chemistry (IQSC), University of São Paulo (USP), São Carlos 13566-590, SP, Brazil; stanislau@iqsc.usp.br
[4] BioMyne-Biotech Innovation and Engineering Ltd., Macau 999078, China; deepamora@bio-myne.com
[5] State Key Laboratory of Quality Research in Chinese Medicine, Science and Technology Building, Macau University of Science and Technology, Avenida Wai Long, Taipa, Macau 999078, China
* Correspondence: coghips@must.edu.mo; Tel.: +853-88972853

Abstract

In this report, we describe the synthesis of two new celastrol derivatives featuring aryl-substituted 1,2,3-triazole fragments attached to the celastrol scaffold via an ester linkage. The target compounds, incorporating 4-methoxyphenyl and *p*-tert-butylphenyl groups, were characterized by ^{1}H and ^{13}C NMR spectroscopy, FTIR, UV-Vis, HRMS, melting point determination, and specific rotation measurements.

Keywords: celastrol; rheumatoid arthritis; triterpenoids; click chemistry; structure–activity relationship

1. Introduction

Celastrol is a pentacyclic quinone methide triterpenoid isolated from *Tripterygium wilfordii Hook. f.* and is one of the most widely studied active compounds in Tripterygium wilfordii. In recent years, as research into its molecular mechanisms has progressed, celastrol has attracted significantly greater attention in pharmaceutical research. A large body of research has demonstrated that celastrol possesses a wide range of pharmacological activities, including anti-inflammatory, antioxidant, anti-tumour, neuroprotective, anti-obesity and immunomodulatory effects [1,2]. These pharmacological activities do not exist in isolation from one another but are closely linked to celastrol's interference with several key signalling pathways and cellular regulatory networks. Celastrol acts on several key molecular targets closely associated with inflammatory responses, cellular stress, protein homeostasis and cell survival. For example, celastrol modulates classical inflammatory signalling pathways such as NF-κB, thereby influencing the expression of inflammatory factors, chemokines and molecules involved in matrix degradation. It can also interfere with the function of the Hsp90-Cdc37 chaperone complex, thereby affecting the stability of related signalling proteins and the cellular stress adaptation process [3]. Furthermore, celastrol's regulation of SERCA suggests that it may be involved in processes such as intracellular Ca^{2+} homeostasis, endoplasmic reticulum stress and autophagy, mechanisms which are of significant importance in both inflammatory and autoimmune diseases [4]. In

Check for updates

Academic Editor: Jiangjiang Tang

Received: 16 April 2026
Revised: 12 May 2026
Accepted: 29 May 2026
Published: 3 June 2026

Copyright: © 2026 by the authors. Licensee MDPI, Basel, Switzerland. This article is an open access article distributed under the terms and conditions of the Creative Commons Attribution (CC BY) license.

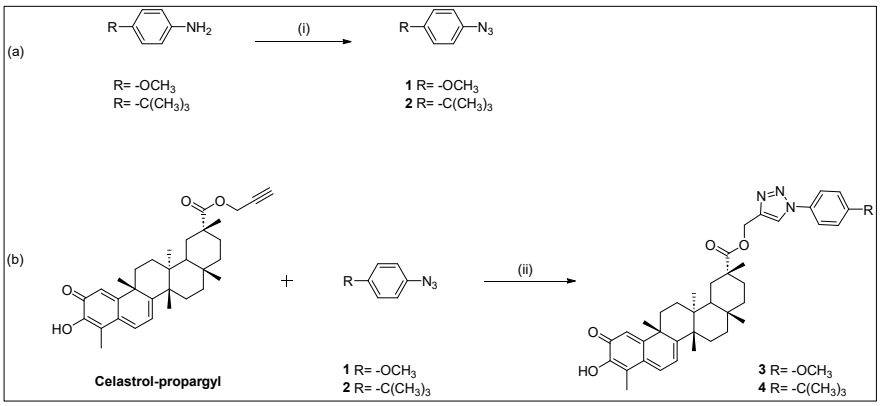
other words, the action of celastrol does not rely on a single target but rather exerts its overall pharmacological effects through synergistic intervention across multiple pathological pathways. It is for this reason that celastrol has demonstrated significant research value in diseases with complex mechanisms, such as inflammatory and autoimmune disorders, with rheumatoid arthritis (RA) currently being one of the primary areas of focus [5].

RA is a chronic, autoimmune inflammatory disease characterized primarily by persistent synovial inflammation that progressively leads to cartilage destruction and bone erosion. The pathological process of RA is not determined by a single inflammatory factor but rather results from the combined action of various immune cells, synovial cells and inflammatory mediators. Among these, fibroblast-like synoviocytes (FLSs) play a crucial role in the ongoing progression of the disease [6,7]. Abnormally activated RA-FLSs exhibit changes such as enhanced proliferation, anti-apoptotic properties, and increased migration and invasive capabilities, whilst continuously releasing inflammatory factors, chemokines and matrix metalloproteinases, thereby further exacerbating local inflammatory responses and joint tissue damage [8]. Concurrently, processes such as NF-κB-related inflammatory signalling, alterations in Ca^{2+} homeostasis, abnormal autophagy and osteoclast activation also contribute to the onset and progression of RA [9–11]. For this reason, RA is best understood from the perspective of multi-pathway regulation, and therapeutic research should focus on small molecules capable of simultaneously targeting inflammation, abnormal synovial activation and tissue destruction.

This also implies that the treatment of RA is not well suited to relying on a single target for explanation or intervention; rather, it requires a focus on small molecules capable of simultaneously influencing multiple pathological pathways. From this perspective, the reason celastrol has attracted attention in RA research is not merely because of its anti-inflammatory activity, but more importantly because its mode of action corresponds to the complex pathological processes underlying RA.

Based on the aforementioned research, there remains scope for further structural optimization of celastrol, particularly with regard to more targeted modulation of its biological activity whilst retaining its anti-RA activity. The C29 carboxylic acid site of celastrol is a suitable location for derivatization [12–14]; modification at this site not only preserves the integrity of the parent core framework but also facilitates the introduction of different types of functional moieties [12,15]. Furthermore, both structures containing an anisidine moiety and those containing a triazole moiety have demonstrated promising activity, suggesting that the nature of the aromatic substituents and the triazole linker itself may influence the activity. Based on this approach, this study further selected two types of aromatically substituted triazole moieties for incorporation into the celastrol skeleton: one is *p*-methoxyphenyl-triazole, primarily used to retain the structural features associated with anisidine from previous studies; the other is *p*-tert-butylphenyl-triazole, which is mainly used to investigate the effects of increased hydrophobicity and larger molecular volume on molecular activity. This design approach allows for a preliminary comparison of the effects of different aromatic ring substitution patterns on biological activity within the same core structure and also provides a reference for subsequent structure–activity relationship (SAR) analysis.

This study describes the synthesis of new celastrol derivatives whose scaffold has been linked to bearing aryl-substituted 1,2,3-triazole moieties, including *p*-methoxyphenyl and *p*-tert-butylphenyl-substituted analogues (Scheme 1), which were designed and fully characterized by NMR, IR, UV-Vis, and elemental analyses.



Scheme 1. Synthesis of aryl azides **1**–**2** and celastrol-based aryl-substituted 1,2,3-triazole derivatives **3**–**4**. (**a**) Synthesis of 4-methoxyphenyl azide **1** and 4-tert-butylphenyl azide **2** from the corresponding anilines. (i) Tert-butyl nitrite, t-BuOH/H_2O (*v*/*v* 9:2), NaN_3, 50 °C stirred 4 h. (**b**) Synthesis of celastrol derivatives **3** and **4** bearing *p*-methoxyphenyl and *p*-tert-butylphenyl-substituted 1,2,3-triazole moieties. (ii) 1:1 *v*/*v* t-BuOH/H_2O, $CuSO_4$, 65 °C for 4 h. For **1** and **3**, R = 4-methoxyphenyl; for **2** and **4**, R = 4-tert-butylphenyl.

2. Results and Discussion

The synthetic route to the target celastrol derivatives **3** and **4** is outlined in Scheme 1. The preparation was initiated by the synthesis of the aryl azide intermediates **1** and **2** from the corresponding para-substituted aniline precursors. Using tert-butyl nitrite and sodium azide in t-BuOH/H_2O at 50 °C, 4-methoxyphenyl azide **1** and 4-tert-butylphenyl azide **2** were obtained in 85.5% and 78.4% yields [16,17] (Scheme 1a). These azides were subsequently employed in the $CuSO_4$ sodium ascorbate-mediated azide-alkyne cycloaddition with celastrol-propargyl to furnish the target celastrol derivatives **3** and **4** in 73% and 33% yields (Scheme 1b). Celastrol-propargyl was synthesized from celastrol by C29 esterification with propargyl bromide following a previously reported procedure, with minor modifications, and was used as the alkyne precursor in the CuAAC reaction [18].

The structures of **3** and **4** were confirmed by ^{1}H and ^{13}C NMR spectroscopy, together with IR, UV-Vis, and elemental analyses.

For **3**, the ^{1}H NMR spectrum showed a characteristic singlet at δ 7.83 (1H) attributable to the triazole proton. The para-substituted *p*-methoxyphenyl ring was supported by proton resonances at δ 7.47–7.41 (2H) and 6.94–6.90 (2H), while the methoxy group appeared as a singlet at δ 3.85 (3H). In addition, the linker methylene group was observed as a pair at δ 5.21 and 5.13 (J = 12.6 Hz, 2H total), consistent with a non-equivalent OCH_2 environment adjacent to the newly formed triazole-containing side chain. The preserved celastrol framework was further supported by the characteristic downfield resonances at δ 6.95, 6.50, and 6.28, together with multiple methyl signals in the high-field region. In the ^{13}C NMR spectrum of **3**, the signal at δ 169.93 was assigned to the ester carbonyl carbon, whereas the resonances at δ 159.98, 57.48, and 55.72 supported the presence of the anisole-type aryl substituent and the linker methylene carbon. The retained signals at δ 178.46 and 178.45 were consistent with the preserved carbonyl environment of the celastrol core. For IR, the absorption at 2922 cm^{-1} was assigned to aliphatic C-H stretching while the band at 1728 cm^{-1} was consistent with the ester carbonyl group. Additional bands in the 1681–1634 cm^{-1} region were in agreement with the conjugated carbonyl/olefinic framework of the celastrol core, while the absorptions at 1255, 1217, 1155, 1138, 1088, and 1034 cm^{-1} supported the presence of C-O/C-O-C functionalities associated with the ester linkage and the methoxy-substituted aromatic ring. For UV, A strong absorption band was observed in the UV region (approximately 230–280 nm), which can be attributed mainly to π→π* transitions of the aromatic and conjugated framework. In addition, a broader

absorption band was observed in the visible–near region around 420–440 nm, which is consistent with the presence of the quinone methide/conjugated carbonyl chromophore characteristic of the celastrol scaffold.

A similar spectral pattern was observed for **4**. In the ^{1}H NMR spectrum, a singlet at δ 7.90 (1H) supported the presence of the triazole proton, while the aromatic region showed signals consistent with the *p*-tert-butylphenyl substituent. The characteristic tert-butyl group appeared as a singlet at δ 1.35 (9H), and the linker methylene resonance was observed at δ 5.16 (2H). The proton resonances at δ 6.57 and 6.31, together with aliphatic methyl proton resonances in the high-field region, again supported retention of the celastrol skeleton. In the ^{13}C NMR spectrum, the ester carbonyl carbon was observed at δ 169.96, while the linker methylene carbon appeared at δ 57.56. The signals at δ 34.89 and 31.70/31.40 were in good agreement with the quaternary carbon and methyl carbons of the tert-butyl group. As in **3**, the resonances at δ 178.52 and 178.42 supported preservation of the parent celastrol carbonyl framework. Taken together, these spectroscopic data confirmed the successful synthesis of the two target celastrol derivatives. For IR, strong absorptions at 1763 and 1736 cm^{-1} confirmed the presence of carbonyl functionalities, and the bands observed in the 1686–1618 cm^{-1} region were likewise consistent with the preserved conjugated celastrol framework. The signals at 1570–1508 cm^{-1} and 1466–1400 cm^{-1} were compatible with aromatic skeletal vibrations and alkyl-substituted aryl features. The UV-Vis spectrum of **4** also showed two main absorption regions. An intense band appeared in the UV region (approximately 230–270 nm), which is consistent with $\pi \rightarrow \pi^*$ transitions arising from the aromatic and conjugated structural elements of the molecule. A broader absorption band was likewise observed in the visible–near region around 420–440 nm, indicating that the quinone methide/conjugated carbonyl chromophore of the celastrol core was retained after derivatization. Compared with **3**, the spectral profile of compound 4 may reflect the different electronic contribution of the *p*-tert-butylphenyl substituent.

Although **3** and **4** share the same celastrol core and triazole-containing side chain, they differ in the para-substituent of the terminal phenyl ring, which allows a preliminary comparison of substituent effects. **3,** bearing a *p*-methoxyphenyl group, may be regarded as an extension of the anisidine-related structural feature reported previously, while **4**, containing a *p*-tert-butylphenyl group, was designed to probe the influence of increased hydrophobicity and steric bulk [19]. At this stage, the current compound pair should be viewed as a preliminary SAR model rather than a definitive optimization outcome. Because the celastrol scaffold and the linker architecture are fixed, the main variable in this small series is the nature of the terminal aromatic substituent. The results obtained from this comparison may therefore serve as a useful basis for subsequent analogue design and deeper mechanistic investigation in RA-related models.

Copies of the ^{1}H NMR, ^{13}C NMR, HRMS, FT-IR, UV-Vis spectra, and other supporting data are provided in the Supplementary Materials.

3. Materials and Methods

Silica gel (FCP 230–400 mesh) was used for column chromatography. Thin-layer chromatography was carried out on Merck precoated silica gel 60 F254 plates and visualized with phosphomolybdic acid, iodine, or a UV–visible lamp.

All chemicals were purchased from Bide Pharmatech., Ltd. (Shanghai, China) and J & K scientific (Hong Kong, China).

^{1}H-NMR and ^{13}C-NMR spectra were collected in $CDCl_3$ at 25 °C on a Bruker Ascend®-600 NMR spectrometer (600 MHz for ^{1}H and 150 MHz for ^{13}C) (Bruker BioSpin GmbH, Rheinstetten, Germany). All chemical shifts were reported in the standard δ notation of parts per million using the peak of residual proton signals of $CDCl_3$ as an internal

reference ($CDCl_3$, δC 77.2 ppm, δH 7.26 ppm). High-resolution mass spectra (HRMS) were measured using electrospray ionization (ESI)The measurements were performed in positive ion mode (interface capillary voltage 4500 V); the mass-to-charge ratio was set from m/z 50 to 3000 Da; and external/internal calibration was conducted using electrospray calibration solution. HRMS analyses were performed by an Agilent 6230 ESI time-of-flight (TOF) mass spectrometer (Agilent Technologies, Santa Clara, CA, USA) with Agilent C18 column (4.6 mm × 150 mm, 3.5 µm). The mobile phase was isocratic (water + 0.01% TFA; CH_3CN) at a flow rate of 0.35 mL/min. The peaks were determined at 254 nm using a UV detector.

UV analysis was performed on a Shimadzu UV-2600 (Shimadzu Corporation, Kyoto, Japan) with a 1 cm quartz cell and a slit width of 2.0 nm. The analysis was carried out using wavelengths in the range of 200–700 nm.

The FT-IR analysis was performed using a Shimadzu IRAffinity-1S (Osaka, Japan) with a frequency range of 4000–500 cm^{-1} equipped with a SPECAC ATR accessory.

Melting points were determined on a Büchi M-560 Automatic Melting Point Apparatus (BÜCHI Labortechnik AG, Flawil, Switzerland).

Optical rotations were measured on a Rudolph Research Analytical Autopol IV-T automatic polarimeter (Rudolph Research Analytical, Hackettstown, NJ, USA) using the sodium D line at 589 nm at 25 °C.

3.1. Synthesis of 1-Azido-4-methoxybenzene (**1**)

4-methoxyaniline (1 eq, 123.15 mg) and tert-butyl nitrite (6 eq, 713.6 µL) were added in 1.1 mL of t-BuOH/H_2O (v/v 9:2). Then, NaN_3 (3 eq) was added to the mixture, which was stirred at 50 °C for 4 h.

Using ethyl acetate to extract the mixture, the organic phase was washed three times with water and three times with saturated saline solution; the organic phase was collected, dried over anhydrous Na_2SO_4, filtered, and concentrated in vacuo to yield the pure product, producing a yield of 85.5%.

The spectral characteristics are consistent with those reported in the literature [20].

3.2. Synthesis of 1-Azido-4-methoxybenzene (**2**)

4-(tert-butyl)aniline (1 eq, 149.23 mg) and tert-butyl nitrite (6 eq, 713.6 µL) were added in 1.1 mL t-BuOH/H_2O (v/v 9:2); then, NaN_3 (3 eq) was added in the mixture and stirred at 50 °C for 4 h. Using ethyl acetate to extract mixture, the organic phase was washed three times with water and three times with saturated saline solution; the organic phase was collected, dried over anhydrous Na_2SO_4, filtered, and concentrated in vacuo to yield the pure product, producing a yield of 78.4%.

The spectral characteristics are consistent with those reported in the literature [21].

3.3. Synthesis of (1-(4-Methoxyphenyl)-1H-1,2,3-triazol-4-yl)methyl (2R,4aS,6aS,12bR,14aS)-10-hydroxy-2,4a,6a,9,12b,14a-hexamethyl-11-oxo-1,2,3,4,4a,5,6,6a,11,12b,13,14,14a,14b-tetradecahydropicene-2-carboxylate (**3**)

Sodium ascorbate (0.4 mol) and 1-azido-4-methoxybenzene (1.2 eq) were added to a solution of celastrol-propargyl (30 mg, 0.06 mmol) in 1:1 v/v t-BuOH/H_2O (6 mL), then $CuSO_4$ (0.2 mol) was added to the solution when all compounds dissolved; the mixture was stirred at 65 °C for 4 h. Using ethyl acetate to extract mixture, the organic phase was washed three times with water and three times with saturated saline solution; the organic phase was collected, dried over anhydrous Na_2SO_4, filtered, and concentrated in vacuo to yield the crude product. Purification was achieved by silica gel column chromatography using dichloromethane/methanol 97:3 as the eluent to afford **3** as a brown solid (28 mg, 73%). The melting point was 167.8–169.3 °C. $[\alpha]_D^{25} = -88$ (c = 0.1 in $CHCl_3$).

^{1}H NMR (600 MHz, $CDCl_3$) δ7.83 (s, 1H), 7.47–7.41 (m, 2H), 6.95 (dd, *J* = 7.1, 1.5 Hz, 1H), 6.94–6.90 (m, 2H), 6.50 (d, *J* = 1.5 Hz, 1H), 6.28 (d, *J* = 7.2 Hz, 1H), 5.21 (d, *J* = 12.6 Hz, 1H), 5.13 (d, *J* = 12.6 Hz, 1H), 3.85 (s, 3H), 2.41 (d, *J* = 15.7 Hz, 1H), 2.18 (s, 3H), 2.10–2.00 (m, 3H), 1.92–1.81 (m, 1H), 1.73–1.64 (m, 3H), 1.64–1.45 (m, 5H), 1.39 (s, 3H), 1.25–1.22 (d, *J* = 10.0 Hz, 2H), 1.22 (s, 3H), 1.18 (s, 3H), 1.08 (s, 3H), 0.99–0.93 (m, 1H), 0.35 (s, 3H).^{13}C NMR (151 MHz, $CDCl_3$) δ178.46, 178.45, 169.93, 164.74, 159.98, 146.10, 142.89, 134.03, 130.18, 127.46, 122.39, 122.03, 119.72, 118.16, 117.18, 114.85, 57.48, 55.72, 45.03, 44.35, 43.02, 40.56, 39.52, 38.39, 36.50, 34.87, 33.46, 33.06, 30.64, 29.95, 29.72, 29.49, 28.71,21.69, 18.57, 14.25, 10.35.

HRMS (ESI$^+$) *m*/*z*: [M+H]$^+$calcd for $C_{39}H_{47}N_3O_5{}^+$638.3588; found 638.3586 (Δ0.0002).

3.4. Synthesis of (1-(4-(Tert-butyl)phenyl)-1H-1,2,3-triazol-4-yl)methyl(2R,4aS,6aS,12bS,14aS)-10-hydroxy-2,4a,6a,9,12b,14a-hexamethyl-11-oxo-1,2,3,4,4a,5,6,6a,9,10,11,12b,13,14,14a,14b-hexadecahydropicene-2-carboxylate (**4**)

Sodium ascorbate (0.4 mol) and 1-azido-4-(tert-butyl) benzene (1.2 eq) were added to a solution of celastrol-propargyl (30 mg, 0.06 mmol) in 1:1 *v*/*v* t-BuOH/H_2O (6 mL), then the $CuSO_4$ (0.2 mol) was added to the solution when all compounds dissolved; the mixture was stirred at 65 °C for 4 h. Using ethyl acetate to extract mixture, the organic phase was washed three times with water and three times with saturated saline solution; the organic phase was collected, dried over anhydrous Na_2SO_4, filtered, and concentrated in vacuo to yield the crude product. Purification was achieved by silica gel column chromatography using dichloromethane/methanol 97:3 as the eluent to afford **4** as a brown solid (13 mg, 33%). The melting point was 168.6–170.1 °C. $[\alpha]_D^{25} = -86$ (c = 0.1 in $CHCl_3$).

^{1}H NMR (600 MHz, $CDCl_3$)δ7.90 (s, 1H), 7.53–7.50 (m, 2H), 7.49–7.46 (m, 2H), 7.02–6.96 (m, 2H), 6.57 (d, *J* = 1.4 Hz, 1H), 6.31 (d, *J* = 7.2 Hz, 1H), 5.16 (d, *J* = 2.6 Hz, 2H), 2.47–2.41 (m, 1H), 2.21 (s, 3H), 2.18–2.12 (m, 2H), 2.08–2.00 (m, 1H), 1.91–1.82 (m, 1H), 1.82–1.75 (m, 2H), 1.74–1.61 (m, 2H), 1.59–1.44 (m, 2H), 1.44 (s, 3H), 1.35 (s, 9H), 1.25 (d, *J* = 5.6 Hz, 7H), 1.17 (s, 3H), 1.09 (s, 3H), 0.46 (s, 3H).

^{13}C NMR (151 MHz, $CDCl_3$)δ178.52, 178.42, 169.96, 164.84, 152.44, 146.15, 143.08, 134.48, 134.08, 127.54, 126.81, 122.06, 120.33, 119.79, 118.24, 117.10, 57.56, 45.13, 44.38, 43.09, 40.57, 39.59, 38.42, 36.51, 34.93, 34.89, 33.55, 32.97, 32.08, 31.70, 31.40, 30.67, 29.85, 28.75, 22.84, 21.80, 18.62, 14.27, 10.45.

HRMS (ESI$^+$) *m*/*z*: [M+H]$^+$calcd for $C_{42}H_{53}N_3O_4{}^+$ 664.4109; found 664.4111 (Δ0.0003).

4. Conclusions

In this study, celastrol was used as a lead skeleton, and structural modifications were carried out at the C29 position to design and synthesize two new aryl-substituted 1,2,3-triazole derivatives, incorporating *p*-methoxyphenyl and *p*-tert-butylphenyl moieties, respectively. The target compounds were prepared via click chemistry and structurally characterized using ^{1}H NMR, ^{13}C NMR, IR, UV-Vis HRMS, melting point determination, and specific rotation measurements; the results indicate that both target molecules were successfully obtained. Overall, this design retains the characteristics of the celastrol core whilst introducing aromatic triazole side chains of clear comparative significance, thereby providing a new class of structures for the further optimization of celastrol.

Supplementary Materials: The following supporting information can be downloaded online: Figure S1. ^{1}H NMR spectrum ($CDCl_3$, 600 MHz) of **3**, Figure S2. ^{13}C NMR spectrum ($CDCl_3$, 150 MHz) of **3**, Figure S3. HSQC spectrum ($CDCl_3$, 600 MHz) of **3**, Figure S4. COSY spectrum ($CDCl_3$, 600 MHz) of **3**, Figure S5. ^{1}H NMR spectrum ($CDCl_3$, 600 MHz) of **4**, Figure S6. ^{13}C NMR spectrum ($CDCl_3$, 150 MHz) of **4**, Figure S7. HSQC spectrum ($CDCl_3$, 600 MHz) of **4**, Figure S8. COSY spectrum ($CDCl_3$, 600 MHz) of **4**, Table S1. ^{1}H and ^{13}C NMR chemical shifts and structure of **3**,

Table S2. ^{1}H and ^{13}C NMR chemical shifts and structure of **4**, Figure S9. IR spectrum of **3**, Figure S10. IR spectrum of **4**, Figure S11. UV spectrum of **3**, Figure S12. UV spectrum of **4**, Figure S13. MASS spectra of **3**, Figure S14. MASS spectra of **4**.

Author Contributions: Conceptualization, P.C.; methodology, Y.X., N.M.P.A., S.B.J., D.A. and P.C.; software, Y.X.; validation, P.C.; formal analysis, Y.X.; investigation, Y.X.; data curation, Y.X.; writing—original draft preparation, Y.X.; writing—review and editing, N.M.P.A., S.B.J., D.A. and P.C.; supervision, P.C.; project administration, P.C.; funding acquisition, P.C. All authors have read and agreed to the published version of the manuscript.

Funding: This research was funded by FDCT grants from Macao Science and Technology University to PC (Project Code:0005/2025/RIA1, 0013/2024/AMR). Funded by The Science and Technology Development Fund, Macau SAR (File no. 0003/2025/NRP) and acknowledgment to SKL Chinese Medicine Laboratory. The authors thank the Amazon Foundation for Studies and Research (FAPESPA) (nº 101/2025) for the financial support. This work was also partially supported by the São Paulo Research Foundation (FAPESP) under Grant No. 2022/03229-8 (SBJ).

Data Availability Statement: Data is contained within the article or Supplementary Materials.

Conflicts of Interest: D.A. has a cooperation with BioMyne-Biotech Innovation and Engineering Ltd.; however, this cooperation is unrelated to the content of the present manuscript and does not influence the work reported herein. The authors declare no conflicts of interest.

Abbreviations

RA	rheumatoid arthritis
FLSs	fibroblast-like synoviocytes
NF-κB	nuclear factor kappa B
Hsp90	heat shock protein 90
Cdc37	cell division cycle 37
SERCA	sarco/endoplasmic reticulum Ca^{2+}-ATPase
SAR	structure–activity relationship

References

1. Cascão, R.; Fonseca, J.E.; Moita, L.F. Celastrol: A Spectrum of Treatment Opportunities in Chronic Diseases. *Front. Med.* **2017**, *4*, 69. [CrossRef]
2. Song, J.; He, G.N.; Dai, L. A comprehensive review on celastrol, triptolide and triptonide: Insights on their pharmacological activity, toxicity, combination therapy, new dosage form and novel drug delivery routes. *Biomed. Pharmacother.* **2023**, *162*, 114705. [CrossRef]
3. Shi, J.; Li, J.; Xu, Z.; Chen, L.; Luo, R.; Zhang, C.; Gao, F.; Zhang, J.; Fu, C. Celastrol: A Review of Useful Strategies Overcoming its Limitation in Anticancer Application. *Front. Pharmacol.* **2020**, *11*, 558741. [CrossRef]
4. Coghi, P.; Ng, J.P.L.; Kadioglu, O.; Law, B.Y.K.; Qiu, A.C.; Saeed, M.E.M.; Chen, X.; Ip, C.K.; Efferth, T.H.; Liu, L.; et al. Synthesis, computational docking and biological evaluation of celastrol derivatives as dual inhibitors of SERCA and P-glycoprotein in cancer therapy. *Eur. J. Med. Chem.* **2021**, *224*, 113676. [CrossRef] [PubMed]
5. Amir Yusri, M.A.; Sekar, M.; Wong, L.S.; Gan, S.H.; Ravi, S.; Subramaniyan, V.; Mat Rani, N.N.I.; Chidambaram, K.; Begum, M.Y.; Ramar, M.; et al. Celastrol: A Potential Natural Lead Molecule for New Drug Design, Development and Therapy for Memory Impairment. *Drug Des. Devel Ther.* **2023**, *17*, 1079–1096. [CrossRef]
6. Fang, Z.; He, D.; Yu, B.; Liu, F.; Zuo, J.; Li, Y.; Lin, Q.; Zhou, X.; Wang, Q. High-Throughput Study of the Effects of Celastrol on Activated Fibroblast-Like Synoviocytes from Patients with Rheumatoid Arthritis. *Genes* **2017**, *8*, 221. [CrossRef]
7. Bartok, B.; Firestein, G.S. Fibroblast-like synoviocytes: Key effector cells in rheumatoid arthritis. *Immunol. Rev.* **2010**, *233*, 233–255. [CrossRef]
8. Li, G.Q.; Zhang, Y.; Liu, D.; Qian, Y.Y.; Zhang, H.; Guo, S.Y.; Sunagawa, M.; Hisamitsu, T.; Liu, Y.-Q. Celastrol inhibits interleukin-17A-stimulated rheumatoid fibroblast-like synoviocyte migration and invasion through suppression of NF-κB-mediated matrix metalloproteinase-9 expression. *Int. Immunopharmacol.* **2012**, *14*, 422–431. [CrossRef]
9. Cascão, R.; Vidal, B.; Carvalho, T.; Lopes, I.P.; Romão, V.C.; Goncalves, J.; Moita, L.F.; Fonseca, J.E. Celastrol Efficacy by Oral Administration in the Adjuvant-Induced Arthritis Model. *Front. Med.* **2020**, *7*, 455. [CrossRef] [PubMed]

10. Wong, V.K.W.; Qiu, C.; Xu, S.W.; Law, B.Y.K.; Zeng, W.; Wang, H.; Michelangeli, F.; Dias, I.R.D.S.R.; Qu, Y.Q.; Chan, T.W.; et al. Ca(2+) signalling plays a role in celastrol-mediated suppression of synovial fibroblasts of rheumatoid arthritis patients and experimental arthritis in rats. *Br. J. Pharmacol.* **2019**, *176*, 2922–2944. [CrossRef] [PubMed]
11. Liang, H.-Y.; Yin, H.-X.; Li, S.-F.; Chen, Y.; Zhao, Y.-J.; Hu, W.; Zhou, R.-P. Calcium-Permeable Channels Cooperation for Rheumatoid Arthritis: Therapeutic Opportunities. *Biomolecules* **2022**, *12*, 1383. [CrossRef]
12. Xie, Y.; Kuan, H.; Wei, Q.; Gianoncelli, A.; Ribaudo, G.; Coghi, P. (2R,4aS,6aS,12bR,14aS,14bR)10-Hydroxy-N-(4-((6-methoxyquinolin-8-yl)amino)pentyl)-2,4a,6a,9,12b,14a-hexamethyl-11-oxo-1,2,3,4,4a,5,6,6a,11,12b,13,14,14a,14b-tetradecahydropicene-2-carboxamide. *Molbank* **2023**, *2023*, M1716. [CrossRef]
13. Ren, Z.; Coghi, P. Exploring medicinal potential and drug delivery solutions of Celastrol from the Chinese "Thunder of God Vine". *Eur. J. Chem.* **2024**, *15*, 194–204. [CrossRef]
14. Yuzhu, G.; Anyanwu, M.; Yang, X.; Zimo, R.; Gianoncelli, A.; Ribaudo, G.; Coghi, P. (2R,4aS,6aS,12bR,14aS,14bR)-N-(2-(2-(2-(2-Azidoethoxy)ethoxy)ethoxy)ethyl)-10-hydroxy-2,4a,6a,9,12b,14a-hexamethyl-11-oxo-1,2,3,4,4a,5,6,6a,11,12b,13,14,14a,14b-tetradecahydropicene-2-carboxamide. *Molbank* **2024**, *2024*, M1800. [CrossRef]
15. Chen, Z.; Leong, K.F.; Coluccini, C.; Coghi, P. 4-(1,3-Dioxoisoindolin-2-yl)butyl(2R,4aS,6aS,12bR,14aS,14bR)-10-hydroxy-2,4a,6a,9,12b,14a-hexamethyl-11-oxo-1,2,3,4,4a,5,6,6a,11,12b,13,14,14a,14b-tetradecahydropicene-2-carboxylate. *Molbank* **2025**, *2025*, M2048. [CrossRef]
16. Das, J.; Patil, S.N.; Awasthi, R.; Narasimhulu, C.P.; Trehan, S. An Easy Access to Aryl Azides from Aryl Amines under Neutral Conditions. *Synthesis* **2005**, *2005*, 1801–1806. [CrossRef]
17. Barral, K.; Moorhouse, A.D.; Moses, J.E. Efficient Conversion of Aromatic Amines into Azides: A One-Pot Synthesis of Triazole Linkages. *Org. Lett.* **2007**, *9*, 1809–1811. [CrossRef] [PubMed]
18. He, Q.-W.; Feng, J.-H.; Hu, X.-L.; Long, H.; Huang, X.-F.; Jiang, Z.-Z.; Zhang, X.-Q.; Ye, W.-C.; Wang, H. Synthesis and Biological Evaluation of Celastrol Derivatives as Potential Immunosuppressive Agents. *J. Nat. Prod.* **2020**, *83*, 2578–2586. [CrossRef] [PubMed]
19. Huang, B.; Ng, J.P.; Zhang, D.; Wang, L.; Yang, J.; Li, Y.; Tan, C.R.; Luo, G.; Chen, Z.; Qin, B.; et al. Celastrol derivatives ameliorate arthritis in AIA rats via modulating calcium signaling. *Phytomedicine* **2025**, *146*, 157110. [CrossRef]
20. Aslam, M.W.; Tabares, L.C.; Andreoni, A.; Canters, G.W.; Rutjes, F.P.J.T.; Van Delft, F.L. 2-Deoxystreptamine Conjugates by Truncation–Derivatization of Neomycin. *Pharmaceuticals* **2010**, *3*, 679–701. [CrossRef]
21. Yadav, D.; Singh, N.; Kim, T.W.; Kim, J.Y.; Park, N.J.; Baeg, J.O. Highly regioselective and sustainable solar click reaction: A new post-synthetic modified triazole organic polymer as a recyclable photocatalyst for regioselective azide-alkyne cycloaddition reaction. *Green Chem.* **2019**, *21*, 2677–2685. [CrossRef]

Disclaimer/Publisher's Note: The statements, opinions and data contained in all publications are solely those of the individual author(s) and contributor(s) and not of MDPI and/or the editor(s). MDPI and/or the editor(s) disclaim responsibility for any injury to people or property resulting from any ideas, methods, instructions or products referred to in the content.